Energies of Molecular Interactions from Bragg Diffraction Data

M. A. Spackman,† H. P. Weber,‡ and B. M. Craven*

Contribution from the Department of Crystallography, University of Pittsburgh, Pittsburgh, Pennsylvania 15260. *Received March 30, 1987*

Abstract: Energies are calculated for the interaction of pairs of molecules taken from six crystal structures (imidazole, 9-methyladenine, cytosine monohydrate, urea, the 1:1 complex of thiourea with parabanic acid, and alloxan). A simple model is used where the total energy is $E_{es} + E_{pen} + E_{rep} + E_{disp}$. The last two terms involve a consistent set of exp-6 atom–atom potentials derived via electron-gas theory. The first two are classical terms derived from the experimental charge density distribution, which is partitioned by means of a multipole expansion about atomic centers. When accurate low-temperature high-resolution X-ray and neutron diffraction data are available, electrostatic energies for H-bonding and molecular stacking interactions can be highly significant in terms of their estimated standard deviations. The model is unsuccessful when applied to alloxan where the molecules form a number of unusually short C=O- - -C interactions.

Over the past decade, it has become evident that X-ray and neutron diffraction data can be used for the accurate determination of the electron density distribution in simple molecular crystals. In these studies, emphasis has been in mapping the deformation charge density obtained from the total density by subtracting the contribution of an array of neutral spherical atoms. However, given the experimental parameters that describe the deformation charge density, other electrostatic properties can be derived, such as molecular dipole moments, the electrostatic potential, or the electrostatic energy of interaction of molecules in crystals. Furthermore, these electrostatic properties can be derived for molecules or finite groups of molecules removed from the crystal structure and assembled in any required arrangement. Presently, we describe calculations of the energies of molecular interactions based on experimental charge density studies carried out in this laboratory. They involve six crystal structures of biological interest.

Similar studies have already been reported, notably by Berkovitch-Yellin, Leiserowitz, and co-workers.[1-4] Their work was based on low-temperature X-ray diffraction data for the crystal complex of acetamide with allenedicarboxylic acid,[5] and also for 1,3-diethylbicyclobutane-*exo*,*exo*-2,4-dicarboxylic acid[6] and α-glycine,[7] and made use of the atomic partitioning scheme for the molecular charge density which was introduced by Hirshfeld.[8] Assuming transferability of fragment moments, results were used to provide information on crystal packing in a large number of amide and carboxylic acid structures and to calculate the habit of organic crystals with known crystal structures. Despite the widespread application of these methods, the results are limited by several factors. One is the absence of neutron data for precisely locating the hydrogen atoms, except for α-glycine, where such data were used. Another is the lack of consideration of experimental standard deviations in the assumed electron distributions. Finally, the experimental electron distributions were used to calculate electrostatic energies, which were coupled with estimates of other terms via empirical exp-6 or 6-12 atom–atom potentials. These potentials were not used consistently in all applications, sometimes being modified for the problem at hand. Also, the treatment of the hydrogen bond was unsatisfactory.

Moss and Feil[9] have derived intermolecular electrostatic energies from room-temperature X-ray diffraction data on pyrazine. They considered two molecules at large separation and varied their relative orientations. Only qualitative agreement with ab initio calculations was obtained, probably due to the relatively low quality of the data. Better results were obtained in a succeeding model calculation[10] with use of theoretical structure factors. The experimental analysis, like those described above, did not report estimated errors in the derived electrostatic energies.

The work that we describe uses a model for molecular interactions proposed by Spackman[11-13] and tested successfully for a variety of simple hydrogen-bonded dimers ranging in complexity up to systems involving formic acid and formamide. In these systems, the charge density distribution came from high quality ab initio wave functions for the component molecules. The model includes a consistent set of exp-6 atom–atom potentials that were derived via electron-gas theory. We now extend the application of this model by substituting the charge density parameters from crystallographic studies for those that were previously derived theoretically.

The Model and Its Application

(a) The Model. Although the model for intermolecular interactions has been discussed at length elsewhere,[11-13] we review here its major features and assumptions. The model is designed to provide a simple but quantitative description of the nonbonded interaction between molecules. Its major assumptions are the following: (i) The interacting systems are not perturbed by the interactions. (ii) The electron density $\rho(r)$ and electrostatic potential $\phi(r)$ of each monomer can be described by the promolecule (an assembly of neutral spherical atoms) plus the sum of electrostatic moments of the component atom-like fragments, describing local asphericity. (iii) The electrostatic energy is given by the classical interaction between $\rho(r)$ of one monomer and $\phi(r)$ of the other. (iv) Short-range repulsion and long-range dispersion energies can be approximated by an atom–atom potential derived from electron-gas calculations of atom pairs.[11] (v) A hydrogen bond can be described by omitting the atom–atom potential terms between the proton and its acceptor. The total interaction energy is then written

$$E = E_{es} + E_{pen} + E_{rep} + E_{disp} \quad (1)$$

† Present address: Department of Chemistry, The University of New England, Armidale, New South Wales, 2351 Australia.

‡ Present address: Institut de Cristallographie, Université de Lausanne, B.S.P., CH-1015 Lausanne-Dorigny, Switzerland.

(1) Berkovitch-Yellin, Z. *J. Am. Chem. Soc.* **1985**, *107*, 3239-3253.
(2) Berkovitch-Yellin, Z.; Leiserowitz, L. *J. Am. Chem. Soc.* **1980**, *102*, 7677-7690.
(3) Berkovitch-Yellin, Z.; Leiserowitz, L. *J. Am. Chem. Soc.* **1982**, *104*, 4052-4064.
(4) Berkovitch-Yellin, Z.; van Mil, J.; Addadi, L.; Idelson, M.; Lahav, M.; Leiserowitz, L. *J. Am. Chem. Soc.* **1985**, *107*, 3111-3122.
(5) Berkovitch-Yellin, Z.; Leiserowitz, L.; Nader, F. *Acta Crystallogr., Sect. B* **1977**, *33*, 3670-3677.
(6) Eisenstein, M.; Hirshfeld, F. L. *Acta Crystallogr., Sect. C* **1983**, *39*, 61-75.
(7) Legros, J.-P.; Kvick, Å. *Acta Crystalogr., Sect. B* **1980**, *36*, 3052-3059.
(8) Hirshfeld, F. L. *Theoret. Chim. Acta* **1977**, *44*, 129-138.
(9) Moss, G.; Feil, D. *Acta Crystallogr., Sect. A* **1981**, *37*, 414-421.
(10) Feil, D.; Moss, G. *Acta Crystallogr., Sect. A* **1983**, *39*, 14-21.
(11) Spackman, M. A. *J. Chem. Phys.* **1986**, *85*, 6579-6586.
(12) Spackman, M. A. *J. Chem. Phys.* **1986**, *85*, 6587-6601.
(13) Spackman, M. A. *J. Phys. Chem.* **1987**, *91*, 3179-3186.

0002-7863/88/1510-0775$01.50/0

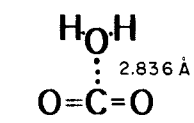

Figure 1. Observed configuration for H_2O–CO_2.

where the terms have been discussed in detail by Spackman.[11-13]

For the purposes of the present work, we emphasize the importance of assumption v, which allows the successful description of the hydrogen bond. As shown by Spackman,[13] the neglected repulsive part of the atom–atom potential for the hydrogen atom and its acceptor correlates with the sum of charge transfer and polarization energies derived via a partitioning of ab initio energies. We therefore assert that the model accounts for these terms, although not in an explicit way. More work needs to be done on the relationship between short-range repulsive and charge-transfer/polarization energies in hydrogen bonding.

(b) The Description of Close C=O···C Contacts. We wish to extend the applicability of the model to describe non-hydrogen-bonded close intermolecular contacts of the sort observed in the crystal structures of parabanic acid[14] and alloxan.[15] These structures have unusually short C···O distances (2.73 Å in alloxan, 2.77 Å in parabanic acid) which are much less than the usual sum of van der Waals radii (3.1 to 3.2 Å). Such interactions are not particularly well understood,[16-19] but we must allow for their inclusion in our simple model if we hope to understand the crystal structures of these systems.

A simpler example of the O···C close contact is observed in the CO_2–H_2O gas-phase dimer,[20] which has a planar (C_{2v}) "anti-hydrogen-bonded" structure (Figure 1), with R(O···C) = 2.836 Å. At such a short separation, the C···O exp-6 atom–atom potential terms in our model are E_{rep} = 9.9 kJ mol^{-1} and E_{disp} = −3.3 kJ mol^{-1}, a net repulsion. It is likely that if we neglect these terms in the same manner as our hydrogen bonding assumption, we can account for an attractive, charge-transfer-type of interaction. From the ab initio partitioning procedure of Reed et al.,[21] the charge-transfer energy in the CO_2–H_2O complex has a magnitude of −11.2 kJ mol^{-1} at a C···O separation of 2.79 Å, and an exponential dependence of the form $E_{ct} = \alpha - e^{-2.99r}$ (r in Å). This means that at R(O···C) = 2.836 Å, $E_{ct} \sim -9.7$ kJ mol^{-1}, a value very close to E_{rep} obtained from our exp-6 potentials.

To see in more detail that the omission of the exp-6 potential for the two atoms involved in a non-hydrogen-bonded interaction can produce realistic results for complexes with these short C···O contacts, we performed calculations on the CO_2–H_2O complex, using moments of the electron density given by Buckingham and Fowler.[22] The method of the calculation is described by Spackman.[13] The model predicts the planar complex to be lowest in energy with R(O···C) = 2.77 Å, close to the experimental value of 2.836 Å. The binding energy of 10.1 kJ mol^{-1} is essentially the same as the value 13.1 kJ mol^{-1} predicted by ab initio theory (6-31G* basis; Reed et al.[21]) and 11.9 kJ mol^{-1} predicted by intermolecular perturbation theory.[23] Moreover, the barrier to rotation of the water molecule about the symmetry axis is 3.6 kJ mol^{-1} (assuming R(C···O) fixed), in accord with the experimental estimate[20] of 3.8 ± 0.9 kJ mol^{-1}.

It therefore appears that neglect of the atom–atom potential terms between C and O atoms involved in close intermolecular contacts can provide a realistic description of the interaction in these systems. It does not, however, provide much insight about the origins of the interaction; that is a far more complex problem. Our aim here is merely to describe them within the limits of our simple model of intermolecular interactions.

(c) Application to Experimental Electron Densities. Very few changes need to be made from the original applications of the model[11-13] in order to apply it to experimental molecular electron densities.

The pseudoatom multipole expansion used to derive electron distributions from the diffraction data has been described in detail elsewhere.[24,25] The result of such a procedure is an atom-centered multipole expansion of the electron density for each of the molecules in the crystal. For the evaluation of E_{es}, this expansion can be conveniently summarized by the atomic multipole moments.

We write the electron density of a pseudoatom at a point with spherical coordinates (r,θ,ϕ) with respect to the atom center,[26]

$$\rho(r,\theta,\phi) = \rho_{at}(r) + \sum_{l=0}^{L}\sum_{m=0}^{l} C_{lm\pm}(r)R_{nl}(r)Y_{lm\pm}(\theta,\phi)$$

where $\rho_{at}(r)$ is a spherical atom electron density. The remaining terms, which describe the pseudoatom asphericity, have weights $C_{lm\pm}$ which are determined by a least-squares fit to the experimental diffraction data. Least-squares fitting also provides $\sigma(C_{lm\pm})$ from which the errors in E_{es} can be estimated. The radial functions in the equation above are given by

$$R_{nl}(r) = (4\pi)^{-1}\frac{\alpha^{n+3}}{(n+2)!}r^n \exp(-\alpha r)$$

Since the angular functions are orthonormal spherical harmonics, it is straightforward to derive moments of the form $\langle r^l Y_{lm\pm}(\theta,\phi)\rangle$, which are then used for the evaluation of E_{es}. For molecules that have been rotated from the orientation in the asymmetric unit of the crystal, we first transform $C_{lm\pm}$ and the spherical harmonics for each pseudoatom according to the method outlined by Cromer et al.[27] The computation of E_{es} is approximated in terms of electrostatic moments with spherical harmonics converted to a Cartesian tensor representation.[28] Expressions for the pseudoatom moments then become

$$-\int r^l Y_{lm\pm}(\theta,\phi)\rho(r,\theta,\phi)\,d\tau = -C_{lm\pm}\int_0^\infty r^{l+2}R_{nl}(r)\,dr \times \int\int [Y_{lm\pm}(\theta,\phi)]^2 \sin\theta\,d\theta\,d\phi = -C_{lm\pm}\frac{(n+l+2)!}{(n+2)!}\frac{(1+\delta_{m,0})}{\alpha^l(4l+2)}\frac{(l+m)!}{(l-m)!}$$

where the minus sign arises from the fact that the electron density, although conventionally positive, has a negative charge. The nuclear charges are incorporated into the monopole term, which becomes the net charge on the pseudoatom. For the computation of E_{es} and dipole and quadrupole moments of the molecules, it is essential to rescale all point charges to obtain neutral molecules.

Multipole expansions considered in this work extend up to the octopole level on heavy atoms (C, N, O, S), but only up to quadrupoles on hydrogens. All moment–moment interactions are calculated explicitly, including those involving octopoles. In this manner, the expansion of E_{es} as a power series in R^{-n} contains terms up to R^{-7}. The parameters for the repulsion and dispersion terms are taken from Spackman.[11] Parameters appropriate to a standard molecular H atom are selected for H.

(14) Craven, B. M.; McMullan, R. K. *Acta Crystallogr., Sect. B* **1979**, *35*, 934–945.
(15) Swaminathan, S.; Craven, B. M.; McMullan, R. K. *Acta Crystallogr., Sect. B* **1985**, *41*, 113–122.
(16) Bolton, W. *Nature (London)* **1964**, *201*, 987–989.
(17) Pullman, B. *Acta Crystallogr.* **1964**, *17*, 1074–1075.
(18) Prout, C. K.; Wallwork, S. C. *Acta Crystallogr.* **1966**, *21*, 449–450.
(19) Bürgi, H. B.; Dunitz, J. D.; Shefter, E. *Acta Crystallogr., Sect. B* **1974**, *30*, 1517–1527.
(20) Peterson, K. I.; Klemperer, W. *J. Chem. Phys.* **1984**, *80*, 2439–2445.
(21) Reed, A. E.; Weinhold, F.; Curtiss, L. A.; Pochatko, D. J. *J. Chem. Phys.* **1986**, *84*, 5687–5705.
(22) Buckingham, A. D.; Fowler, P. W. *Can. J. Chem.* **1985**, *63*, 2018–2025.
(23) Hurst, G. J. B.; Fowler, P. W.; Stone, A. J.; Buckingham, A. D. *Int. J. Quantum Chem.* **1986**, *29*, 1223–1239.
(24) Stewart, R. F. *Acta Crystallogr., Sect A* **1976**, *32*, 565–574.
(25) Craven, B. M.; Weber, H.-P. *The POP Least-Squares Refinement Procedure*; Technical *Report*, Department of Crystallography, University of Pittsburgh, Pittsburgh, PA, 1982.
(26) Epstein, J.; Ruble, J. R.; Craven, B. M. *Acta Crystallogr., Sect. B* **1982**, *38*, 140–149.
(27) Cromer, D. T.; Larson, A. C.; Stewart, R. F. *J. Chem. Phys.* **1976**, *65*, 336–349.
(28) Buckingham, A. D. In *Intermolecular Interactions: From Diatomics to Biopolymers*; Pullman, B., Ed.; Wiley: New York, 1978; pp 1–67.

Table I. Molecular Dipole Moments with Esds (D)[a]

molecule	$\|\mu\|$ crystal	$\|\mu\|$ solution or gas
imidazole	4.8 (0.6)	4.0 (1)[b]
9-methyladenine	1.8 (1.0)	~3.0[c]
cytosine (in hydrate)	8.0 (1.4)	~7[d]
water (D_2O in cytosine monohydrate)	2.3 (0.3)	1.8[e]
urea	5.4 (0.5)	3.8,[f] 4.2,[g] 4.6[h]
thiourea (in crystal complex)	5.2 (1.8)	4.9[h]
parabanic acid (in crystal complex)	4.0 (1.6)	
alloxan	0.2 (1.0)	

[a] values of $|\mu|$ (D) from diffraction data are derived from pseudoatom monopole and dipole population parameters,[29] the former scaled if necessary, to give zero net charge on the molecule. Esds are calculated with respect to the molecular center of mass as origin. The orientation of $\vec{\mu}$ is shown in Figures 2 through 7. [b] Reference 30 (solution). [c] References 31 and 32 (solution). [d] Reference 33 (estimated from solution values for methylated cytosines). [e] Reference 34 (microwave). [f] Reference 35 (microwave). [g] Reference 36 (solution). [h] Reference 37 (solution).

We can perform two distinct types of calculation. First, we can obtain the interaction between a central molecule and each of selected neighbors in the crystal structure. In this manner we can estimate the magnitude of the strongest interactions in the crystal. Alternatively, two molecules can be removed from the crystal and rearranged if required, and then the intermolecular geometry can be relaxed. A comparison of the results allows us to deduce whether the crystal configuration is near optimum. In principle, using molecules from different crystals, we could explore pair interactions that are not observed in any crystal structure.

Typical calculations of energies and esds for a given dimer configuration require less than 10 min of VAX750 computing time.

Results

As a test of the quality of the charge density distributions that were used to obtain E_{es}, we calculated the dipole moment for the individual molecules involved. Each dipole moment (Table I) was obtained from the parameters of a multipole crystal structure refinement, following the procedure of Stewart.[29] Details of these structure refinements are to be found in the charge density studies that are cited below. From Table I, it is seen that the dipole moments from diffraction data agree satisfactorily with the available values determined by other methods, although our values tend to be larger. The difference may arise because a molecule, after it has been extracted from a crystal structure, retains any enhanced polarization due to the interaction with its crystal environment. The effect is consistent with observations from microwave spectroscopy and ab initio theoretical calculations on hydrogen-bonded dimers, which show that the dipole moment of the dimer is frequently greater (by as much as 1 D) than the vector sum of the monomer moments.

(a) Imidazole. We use the multipole refinement at 103 K of Epstein et al.[26] and the neutron coordinates of McMullan et al.[38] Table II gives the energies for the closest intermolecular interactions in the crystal. The crystal structure (Figure 2) is characterized by strings of hydrogen-bonded molecules along *c*, stacked such that each N(1) atom is superimposed on another at a separation of 3.42 Å. The experimental electron density for imidazole gives $|\mu| = 4.8$ (0.6) D for the dipole moment, close to the solution value of 4.0 D,[30] and greater than a minimal basis calculation of

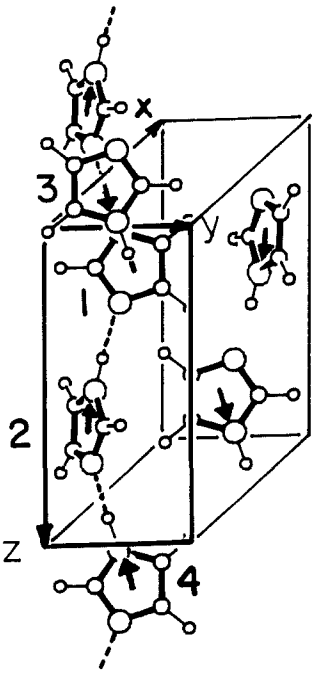

Figure 2. The crystal structure of imidazole, $C_3H_4N_2$, space group $P2_1/c$. The unit cell is bounded by solid lines. Circles in order of decreasing size represent N, C, and H atoms. Hydrogen bonds are shown by dashed lines. The direction of the dipole moment is indicated by arrows originating at the molecular center of mass. The molecules are numbered as explained in Table II.

3.54 D.[46] The direction of μ in the crystal structure is 13 (12)° from the N(3) to N(1) vector, in agreement with the theoretical result which places it within 2° of this vector.[46] It is interesting that a simplified calculation for the imidazole dimer[47] yields a dipole moment enhancement of 0.8 D, which would correspond to a molecular $|\mu| \sim 4.4$ D in the dimer, a value in still better accord with our experimental estimate. We therefore believe that the charge density distribution from diffraction data gives a realistic picture of the polarity of imidazole.

The hydrogen bond energy in the dimer having the crystal geometry is −30 (14) kJ mol^{-1}. This is near the mean of the distribution of theoretical estimates, again at the crystal geometry, of −27.0 kJ mol^{-1},[47] −41.4 kJ mol^{-1} (4-31G) and −36.8 kJ mol^{-1} (STO-3G with no account of basis set superposition error),[48] −39.7

(29) Stewart, R. F. *J. Chem. Phys.* **1972**, *57*, 1664–1668.
(30) Mauret, P.; Fayet, F.-P.; Fabre, M. *Bull. Soc. Chim.* **1975**, 1675–1678.
(31) Bloomfield, V. A.; Crothers, D. M.; Tinoco, I. *Physical Chemistry of Nucleic Acids*; Harper and Row: New York, 1974; p 20.
(32) De Voe, H.; Tinoco, I. *J. Mol. Biol.* **1962**, *4*, 500–517.
(33) Palmer, M. H.; Wheeler, J. R.; Kwiatkowski, J. S.; Lesyng, B. *J. Mol. Struct.* **1983**, *92*, 283–302.
(34) Dyke, T. R.; Muenter, J. S. *J. Chem. Phys.* **1973**, *59*, 3125–3127.
(35) Brown, R. D.; Godfrey, P. D.; Storey, J. *J. Mol. Spectrosc.* **1975**, *58*, 445–450.
(36) Gilkerson, W. R.; Srivastava, K. K. *J. Phys. Chem.* **1960**, *64*, 1485–1487.
(37) Kumler, W. D.; Fohlen, G. M. *J. Am. Chem. Soc.* **1942**, *64*, 1944–1948.
(38) McMullan, R. K.; Epstein, J.; Ruble, J. R.; Craven, B. M. *Acta Crystallogr., Sect. B* **1979**, *35*, 688–691.
(39) Craven, B. M.; Benci, P. *Acta Crystallogr., Sect. B* **1981**, *37*, 1584–1591.
(40) McMullan, R. K.; Benci, P.; Craven, B. M. *Acta Crystallogr., Sect. B* **1980**, *36*, 1424–1430.
(41) Weber, H.-P.; Craven, B. M., manuscript in preparation.
(42) Weber, H.-P.; Craven, B. M.; McMullan, R. K. *Acta Cystallogr., Sect B* **1980**, *36*, 645–649. In the crystal, D was substituted for H except for the C–H groups in cytosine.
(43) Swaminathan, S.; Craven, B. M.; Spackman, M. A.; Stewart, R. F. *Acta Crystallogr., Sect. B* **1984**, *40*, 398–404. Two models (I_x and II_x) were used in describing the charge density for urea. They differ with respect to the values of the exponents used in the pseudoatom radial functions, and hence also in the electron population parameters. The models agree equally well with the X-ray data. Present calculations assuming I_x and II_x gave results agreeing within less than one esd., e.g., the dipole moment has values 5.4 (5) D with I_x and 5.7 (5) D with II_x. In Tables I, II, and III we have chosen to report values based on model I_x in which the radial exponents have the standard values of Hehre et al.: Hehre, W. J.; Stewart, R. F.; Pople, J. A. *J. Chem. Phys.* **1969**, *51*, 2657–2664.
(44) Swaminathan, S.; Craven, B. M.; McMullan, R. K. *Acta Crystallogr., Sect B* **1984**, *40*, 300–306.
(45) Weber, H.-P.; Craven, B. M. *Acta Crystallogr., Sect. B* **1987**, *43*, 202–209.
(46) Del Bene, J. E.; Cohen, I. *J. Am. Chem. Soc.* **1978**, *100*, 5285–5290.
(47) Chojnacki, H.; Lipinski, J. *Adv. Mol. Relax. Processes* **1980**, *18*, 149–155.

Table II. Energies of Interaction (kJ mol^{-1})[a]

second molecule	E_{es}	U	$E_{es} + U$	comment
		Imidazole,[b] Figure 2		
2: $(x, {}^1/_2 - y, {}^1/_2 + z)$	−44 (14)	14	−30	dimer with one H bond
3: $(-x, 1 - y, -z)$	−37 (5)	−3	−40	partial overlap, adjacent ribbons
4: $(x, y, 1 + z)$	−3 (2)	0	−3	second neighbors, same H-bonded ribbon
		9-Methyladenine,[c] Figure 3		
2: $(x, {}^1/_2 - y, {}^1/_2 + z)$	−29 (8)	13	−16	dimer with two H bonds
3: $(x, {}^{-1}/_2 - y, {}^1/_2 + z)$	1 (4)	5	6	dimer with short C—H···N3 distance
4: $(-x, -y, 1 - z)$	15 (10)	6	21	dimer with extensive overlap
		Cytosine Monohydrate (Deuteriated),[d] Figure 4		
2: $(-x, {}^1/_2 + y, {}^1/_2 - z)$	−96 (27)	21	−75	cytosine dimer with two H bonds
3: $(x, {}^1/_2 - y, {}^1/_2 + z)$	42 (16)	−5	37	cytosine dimer with partial overlap
4: $(-x, -y, -z)$	−18 (15)	−2	−20	cytosine dimer with partial overlap
5: (x, y, z)	−42 (20)	19	−23	cytosine with water as H bond donor
6: $(x, {}^1/_2 - y, {}^1/_2 + z)$	−24 (16)	9	−15	cytosine with water as H bond donor
7: $(1 + x, y, z)$	−22 (16)	18	−3	cytosine with water as H bond acceptor
		Urea,[e] Figure 5		
2: $(x, y, 1 + z)$	−50 (14)	7	−43	head-to-tail dimer with 2 H bonds
3: $(y, -x, 1 - z)$	−32 (10)	7	−25	side-by-side antiparallel dimer, 1 H bond
4: $(x, y, 2 + z)$	−5 (3)	0	−5	see Figure 5, a and b
5: $(x, 1 + y, z)$	4 (2)	−2	2	see Figure 5, a and b
6: $(1 + x, 1 + y, z)$	7 (2)	0	7	see Figure 5, a and b
7: $(-1 + x, 1 + y, z)$	4 (1)	0	4	see Figure 5, a and b
8: $(y, -x, 2 - z)$	5 (4)	0	5	see Figure 5, a and b
9: $(y, -x, -z)$	1 (8)	6	7	see Figure 5, a and b
10: $(1 + x, y, 1 + z)$	−1 (3)	0	−1	see Figure 5, a and b
		1:1 Complex, Thiourea with Parabanic Acid,[f] Figure 6		
2: $(1 + x, y, z)$	9 (13)	2	11	hetero dimer with one H bond
3: $(1 + x, y, 1 + z)$	−28 (24)	9	−19	hetero dimer with two H bonds, NH···O
4: $(1 - x, 1 - y, 1 - z)$	−5 (13)	−1	−6	hetero dimer with S overlap on C4—C5
5: (x, y, z)	−32 (14)	14	−18	hetero dimer with NH···S and NH···O
6: $(x, y, -1 + z)$	−1 (9)	2	1	hetero dimer with short S···O
7: $(x, y, 1 + z)$	−44 (21)	8	−36	parabanic acid dimer with one H bond
		Alloxan,[g] Figure 7		
2: $({}^1/_2 - y, {}^1/_2 + x, {}^1/_4 + z)$	0 (2)	−2	−2	dimer with three short C···O distances
3: $({}^1/_2 + y, {}^{-1}/_2 - x, {}^{-1}/_4 + z)$	−6 (4)	1	−5	dimer with two long NH···O distances

[a] Each energy is for a pair of molecules with a configuration as found in the crystal structure. Molecules are numbered as shown in Figures 2–7. Each pair involves molecule 1 which has fractional atomic coordinates (x,y,z) taken from the appropriate reference. The second molecule has atomic coordinates that can be derived by the space group symmetry operation which is given. E_{es} and $U = E_{rep} + E_{pen} + E_{disp}$ are as defined in eq 1. Negative values represent attractive interactions. Esds for E_{es} are given in parentheses. [b] References 26 and 38. [c] References 39 and 40. [d] References 41 and 42. [e] References 43 and 44. [f] Reference 45. [g] Reference 15.

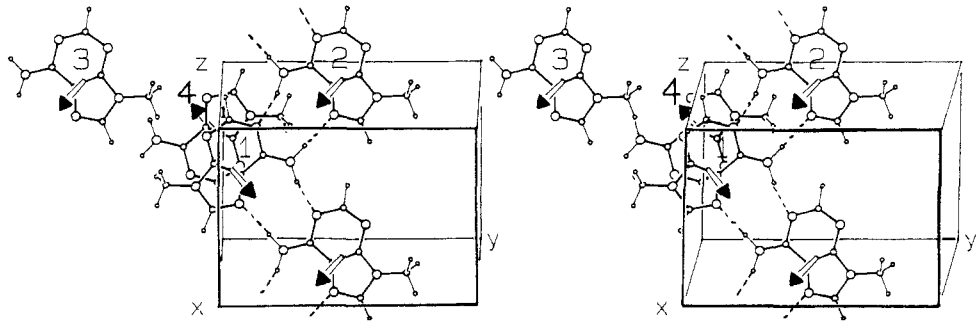

Figure 3. Stereoview[53] of the crystal structure of 9-methyladenine, $C_6H_7N_5$, space group $P2_1/c$. The unit cell contains only molecules for which interactions are listed in Table II.

kJ mol^{-1} (double-ζ),[49] and −30.6 kJ mol^{-1} (semiempirical).[50] The value obtained in chloroform solution, −16.7 ± 3.8 kJ mol^{-1},[51] is also within $\sigma(E_{es})$ of our experimental estimate, although it is much lower than the theoretical values. Another experimental estimate can be obtained from the trimerization energy of −18 kcal mol^{-1},[52] which gives a single hydrogen bond energy of ca. −38 kJ mol^{-1}, in better agreement with our experimental estimate.

Remko[50] estimated the effect of cooperativity in the linear trimer of imidazole to be ca. −1.4 kJ mol^{-1}. From Table II we see that the interaction between molecules separated by c is indeed attractive, with a value of −3.2 (2.0) kJ mol^{-1}.

As we noted in the description of the crystal structure, strings of H-bonded molecules overlap such that the N(1) atom of one molecule is superimposed on N(1) of another at a separation of 3.42 Å. These N atoms are from molecules (1 and 3, Figure 2) related by an inversion and a translation so that their molecular

(48) Brédas, J. L.; Poskin, M. P.; Delhalle, J.; Andfe, J. M.; Chojnacki, H. *J. Phys. Chem.* **1984**, *88*, 5882–5887.
(49) Basch, H.; Krauss, M.; Stevens, W. J. *J. Am. Chem. Soc.* **1985**, *107*, 7267–7271.
(50) Remko, M. *Collect. Czech. Chem. Commun.* **1980**, *45*, 3482–3487.
(51) Wang, S.-M.; Lee, L.-Y.; Chen, J.-T. *Spectrochim. Acta, Part A* **1979**, *35*, 765–771.
(52) Luck, W. A. P. In *The Hydrogen Bond II. Structure and Spectroscopy*; Schuster, P., Zundel, E., Sandorfy, C., Eds.; North-Holland: Amsterdam, 1976; pp 527–562.
(53) Johnson, C. K. ORTEP II, Report ORNL-31588 Oak Ridge National Laboratory, Oak Ridge, TN, 1976.

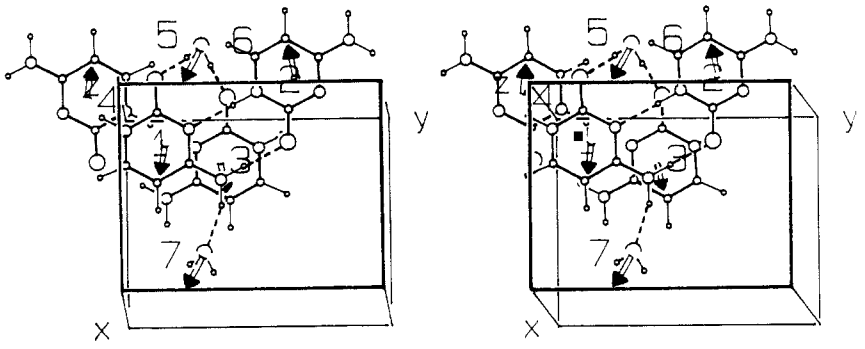

Figure 4. Deuteriated cytosine monohydrate, $C_4H_2D_3N_3O{\cdot}D_2O$, space group $P2_1/c$. Stereoscopic view of the crystal structure.

dipole moments are antiparallel. From Table II we see that their interaction energy is large (−39.7 kJ mol^{-1}) and mostly electrostatic, E_{es} = −36.5 (5.2) kJ mol^{-1}. For comparison, the molecular dipole–dipole energy at this separation is E = −35.7 kJ mol^{-1}, which indicates that the interaction of neighboring ribbons is mostly dipolar in nature. In this case the dispersion energy largely cancels the repulsive energy.

(b) 9-Methyladenine. We use the electron population parameters given by Craven and Benci[39] in their Table 2, and the neutron coordinates of McMullan et al.[40] The crystal structure (Figure 3) consists of sheets of molecules parallel to (100). Two N—H---N hydrogen bonds link adjacent molecules in ribbons along c. The methyl groups lie along edges of these ribbons with close methyl H atom N3 distances 2.524 (2) Å between ribbons in the same sheet. The hydrogen-bonded ribbons are stacked on top of each other along a, with alternating directions. In the crystal, the purine ring system is slightly puckered and the 6-amino group is pyramidal, having H atoms 0.25 and 0.13 Å above the least-squares plane of the purine framework.

We obtain a small molecular dipole moment, 1.8 (1.0) D, directed 38° from the best least-squares plane of the purine framework. However, the orientation of $\vec{\mu}$ is not well determined (σ = 21°). Within the purine plane, the dipole moment has a component 1.4 D directed within 10° of the vector N3–N7 (Figure 3). In several theoretical calculations,[54,55] all based on a planar purine system, values of μ range between 1.1 and 3.0 D with orientations varying by more than 90°.

Table II gives energies for pairs of nearest neighbor molecules in the crystal structure. The energy for the hydrogen-bonded dimer is −16 (8) kJ mol^{-1}. This value compares favorably with that obtained for self-association of 9-ethyladenine in solution (−17 (3) kJ mol^{-1})[56] and with estimates for the adenine–adenine dimer obtained by atom–atom potentials (−14.9 kJ mol^{-1})[57] and quantum mechanically (−23.4 kJ mol^{-1}).[58] In the coplanar dimer (molecules 1 and 3, Figure 3) involving a short methyl H to N3 distance, both the total energy (+6 kJ mol^{-1}) and E_{es} are marginally repulsive. This indicates that the C—H---N interaction should not be regarded as a hydrogen bond. In the dimer (molecules 1 and 4) with extensive molecular overlap, the energy is also repulsive, 20 (10) kJ mol^{-1}. This can be regarded as an effect of the out-of-plane components of the opposed molecular dipoles.

(c) Cytosine Monohydrate. The electron density in the crystal structure was obtained from an X-ray study at 82 K,[41] with hydrogen (deuterium) positions determined from a previous neutron study.[42] In the crystal (Figure 4), cytosine molecules form hydrogen-bonded ribbons extending along b. These ribbons stack along c, with each ribbon linked to the immediate neighbor in the stack by water molecules hydrogen-bonded to the carbonyl groups. A three-dimensional hydrogen-bonding network arises from bonding of amino hydrogens in one stack to the water oxygen in a neighboring stack. An uncommon feature of the hydrogen-bonding pattern is the acceptance of three hydrogen bonds by the carbonyl oxygen.

The quality of the experimental charge distribution can be partially judged by considering the resulting molecular dipole moments. From Table I, the dipole moment for cystosine is $|\mu|$ = 8.0 (1.4) D. The dipole moment is directed at an angle 9 (10)° from the O2=C2 bond. No other experimental values are available for cytosine itself. However, solution measurements of μ for a number of cytosine derivatives indicate a dipole moment of ~7 D.[33] The dipole moment for the D_2O molecule ($|\mu|$ = 2.3 (0.3) D) is slightly greater than the microwave value of 1.84 D for water.[34] In the crystal, $\vec{\mu}$ makes an angle 19 (8)° with the bisector of the D–O–D angle and is directed 13 (7)° from the molecular plane. These deviations from the twofold axis of the isolated molecule are thus of marginal significance in terms of the experimental errors. We conclude that the charge density in the crystal appears to be reliably reproducing the polarity of both molecules.

We observe the strongest interaction [−75 (27) kJ mol^{-1}] for the cytosine dimer (molecules 1 and 2, Figure 4), which has two hydrogen bonds. This energy agrees with the value obtained theoretically[58] for the dimer in the same configuration (−57.4 kJ mol^{-1}).

The stacking interactions between cytosine molecules in the crystal are such that one molecule lies above the hydrogen bonds linking two other molecules in the ribbon at $c/2$ below (Figure 4). Thus we consider two cytosine dimers involving stacking interactions: the dimer involving molecules 1 and 3 has molecular dipole moments approximately parallel, and the other, which involves molecules 1 and 4, has dipole moments antiparallel. From Table II we see that the arrangement with dipoles parallel is strongly repulsive, with a binding energy of 37 (16) kJ mol^{-1}, whereas that with dipoles antiparallel is attractive (−20 (15) kJ mol^{-1}) and partially offsets the repulsive interaction.

The net interaction between layers is attractive because of the hydrogen bonding with water molecules linking cytosine molecules in adjacent layers. From Table II we see that the two cytosine–water interactions where water acts as a proton donor are of approximately the same strength [−24 (20) kJ mol^{-1} and −15 (16) kJ mol^{-1}], whereas the N—H---O(water) hydrogen bond is weaker [−3 (16) kJ mol^{-1}]. These relative strengths correlate well with H---O distances in the structure, the two H---O=C contacts being 1.86 and 1.81 Å, compared to the N—H---O(water) separation of 1.95 Å.

Del Bene has performed ab initio calculations[59] on various water–cytosine complexes, and it is interesting to compare her results with those observed in the crystal structure of cytosine monohydrate. The water–cytosine geometries observed in the crystal have water protons donating to the carbonyl oxygen of cytosine from positions above and below the plane of the cytosine molecule. Del Bene considered only structures with the water oxygen in the cytosine plane. Of those considered by Del Bene, the closest complexes to those observed in the crystal structure

(54) Singh, U. C.; Kollman, P. A. *J. Comput. Chem.* **1984**, *5*, 129–145 and reference therein.
(55) Orbell, J. D.; Solorzano, C.; Marzilli, L. G.; Kistenmacher, T. J. *Inorg. Chem.* **1982**, *21*, 2630–2636.
(56) Kyogoku, Y.; Lord, R. C.; Rich, A. *J. Am. Chem. Soc.* **1967**, *89*, 496–504.
(57) Nash, H. A.; Bradley, D. F. *J. Chem. Phys.* **1966**, *45*, 1380–1386.
(58) Kudritskaya, Z. G.; Danilov, V. I. *J. Theor. Biol.* **1976**, *59*, 303–318.
(59) Del Bene, J. E. *J. Comput. Chem.* **1983**, *4*, 226–233.

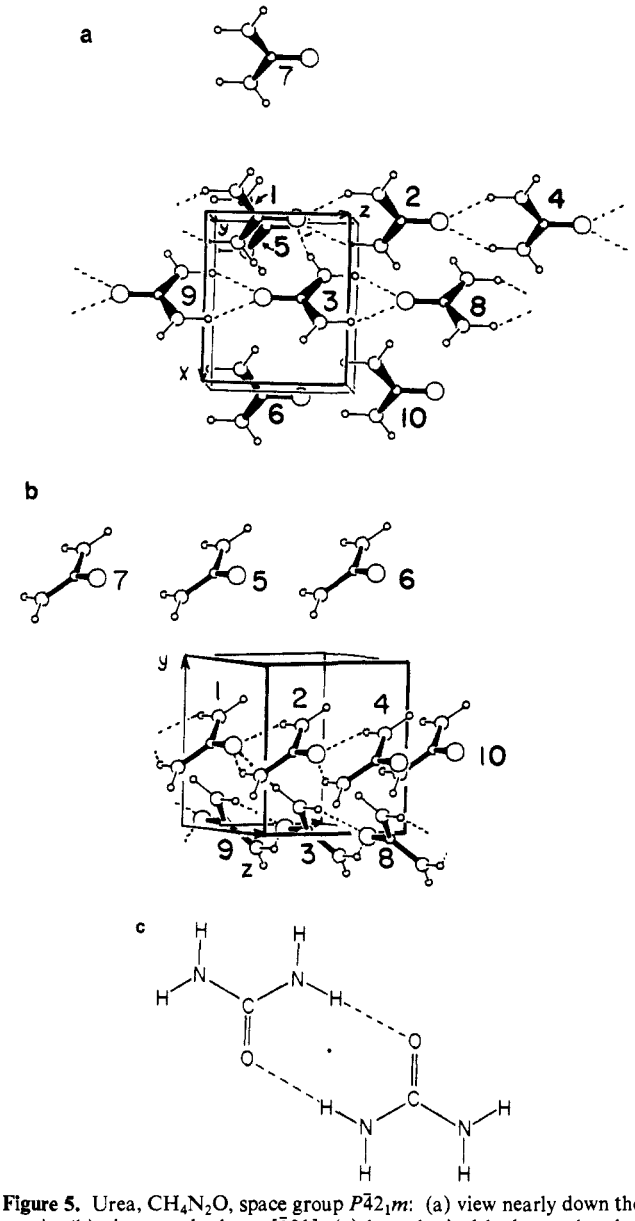

Figure 5. Urea, CH_4N_2O, space group $P\bar{4}2_1m$: (a) view nearly down the y axis; (b) view nearly down [$\bar{1}01$]; (c) hypothetical hydrogen bonded urea dimer.

are B and B′ [see Figure 2 of Del Bene[59]] with R(O--O) distances of 2.78 and 2.82 Å, respectively. These have computed binding energies of 18.4 and 13.8 kJ mol^{-1}, in good agreement with the interaction energies deduced from the crystal structure. The N—H---O(water) complex K considered by Del Bene has a similar configuration to the amino–water hydrogen bond in cytosine monohydrate, where the water oxygen essentially lies in the cytosine ring plane. R(N---O) for complex K is 2.73 Å, compared with 2.92 Å in the crystal. Consequently the binding energy computed for this complex by Del Bene (−23.0 kJ mol^{-1}) is much greater than that observed in the crystal (−3 (16) kJ mol^{-1}).

(d) Urea. Our calculations are based on the charge density analysis of Swaminathan et al.,[43] which in turn makes use of atomic positional and thermal parameters determined by neutron diffraction at 123 K.[44] The crystal structure of urea is simple (Figure 5), consisting of ribbons of doubly hydrogen-bonded molecules arranged in a head-to-tail fashion along c, the plane of each ribbon being perpendicular to adjacent ribbons pointing in the opposite direction along c. Urea appears to provide the only example of a carbonyl O atom accepting four N—H--O hydrogen bonds. The unusual capacity of this O atom as a hydrogen bond acceptor probably accounts for the activity of urea as a protein denaturant.

Table III. Urea, Optimized Hydrogen Bond Dimer Geometries Compared with Crystal Geometries[a]

	crystal structure 123 K	relaxed structure
N—H(1)--O (dimer 1,3)		
N---O	2.998	3.3
H---O	2.009	2.4
∠N—H---O	166.8	147
∠C—O---H	106.2	86
N—H(2)---O (dimer 1,2)		
N---O	2.960	2.9
H---O	2.067	2.0
∠N—H---O	147.6	146
∠C—O---H	146.8	146

[a] Distances are in Å, angles in deg.

The dipole moment for urea in the crystal is 5.4 (5) D, and it is directed from O to C along the O=C bond. The value is somewhat greater than values obtained from the gas (3.8 D) and in solution (4.2 and 4.6 D; see Table I), perhaps due to the extensive hydrogen bonding in the crystal structure. Swaminathan et al.[43] (see their Figure 2c) show small differences consistent with such an effect when comparing the experimental deformation charge density with that of an isolated urea molecule calculated from a 6-31G** wave function. The simple pseudoatom model appears to give a good representation of the charge density in crystals of urea.

As shown in Table II, the urea dimer in the crystal which has the largest interaction energy [−43 (14) kJ mol^{-1}] involves doubly hydrogen-bonded molecules related head-to-tail by the c translation (see molecules 1 and 2; Figure 5). In the dimer (molecules 1 and 3; Figure 5) where there is only one hydrogen bond, the energy [−25 (10) kJ mol^{-1}] is about a half, indicating that all four hydrogen bonds at the urea O atom are approximately of the same strength.

Electrostatic interactions in this lattice are long range, as even the energy of two molecules separated by 2c along c (9.372 Å) is attractive, −5 (3) kJ mol^{-1}. For the other molecular pairs, including interactions with all next-nearest neighbors, most of the energies are repulsive (Table II). This would be expected from the strongly dipolar nature of the urea molecule and the relative orientations of the dipoles in the lattice.

To our knowledge there are no theoretical calculations of urea dimer energies for comparison with our experimental estimates. However, we can easily see if our estimates are at least sensible by computing a cohesive energy for a molecule surrounded by 32 adjacent molecules, using the pair energies in Table II. One-half of this energy is an estimate of the crystal cohesive energy. We obtain a value of −66 (24) kJ mol^{-1}. The observed sublimation energy at 298 K is 88 kJ mol^{-1},[60] and from this Hagler et al.[61] estimated a cohesive energy of ∼93 (6) kJ mol^{-1}. Our estimate of the crystal cohesive energy is surprisingly good, especially since it is only for a small cluster and is probably far from convergence. It indicates that our hydrogen bond energies for urea are realistic.

We have further explored the two different hydrogen-bonded interactions in urea by removing pairs of molecules (1,2) and (1,3) from the lattice and optimizing the relative configuration of each dimer. In Table III, we compare the equilibrium geometries of the hydrogen-bonded dimers with those observed in the crystal at 123 K.[44] Both dimers adopt a configuration close to that of the crystal structure. We conclude that in the crystal structure, there is a compromise in which two strong interactions predominate, one being the head-to-tail arrangement [N—H(2)---O] forming chains along c and the other the [N—H(1)---O] linkages between adjacent antiparallel chains.

(e) The 1:1 Complex of Thiourea and Parabanic Acid. The charge density in this crystal structure was determined from X-ray data collected at room temperature.[45] Consequently, the analysis

(60) Suzuki, K.; Onishi, S.; Koide, T.; Seki, S. *Bull. Chem. Soc. Jpn.* **1956**, *29*, 127-131.
(61) Hagler, A. T.; Huler, E.; Lifson, S. *J. Am. Chem. Soc.* **1974**, *96*, 5319-5327.

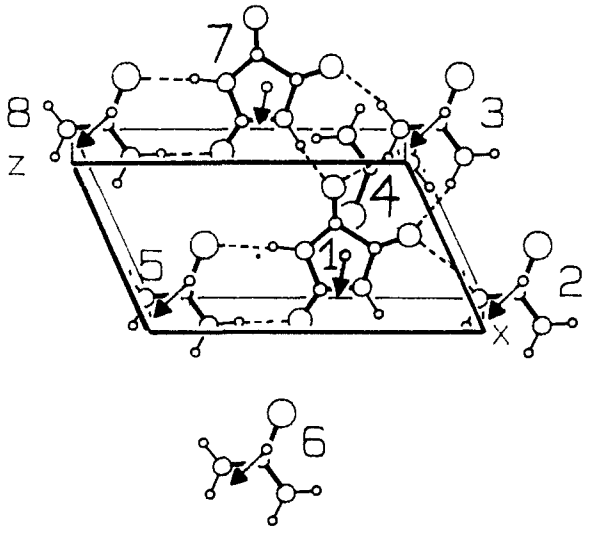

Figure 6. The 1:1 complex of parabanic acid ($C_3H_2N_2O_3$) with thiourea (CH_4N_2S), space group $P2_1/m$.

is of lower accuracy than the others described here, which were based on both X-ray and neutron data collected at low temperature.

The crystal structure (Figure 6) consists of planar sheets of hydrogen-bonded molecules separated by 3.15 Å. Within these sheets, the thiourea S atom forms a hydrogen bond NH---S with parabanic acid (H---S distance 2.25 Å) and also a short S---O distance (3.16 Å). The sheets stack with little molecular overlap except that the S atom of thiourea is near the midpoint of the C–C bond of parabanic acid molecules in adjacent sheets.

As shown in Table I, the dipole moment for thiourea [5.2 (1.8) D] in the crystal complex agrees with the value 4.9 D determined in solution.[37] In the crystal, the dipole moment is directed at an angle 23 (25)° with respect to the S=C double bond and has the same sense as the dipole moment in urea. The dipole moment for parabanic acid is 4.0 (1.6) D, directed at an angle 42 (17)° from the molecular twofold axis. However, with respect to the ureide C=O group in parabanic acid, the sense of the molecular dipole moment is opposite from that of urea itself. In the crystal complex, molecules of thiourea and parabanic acid within the same hydrogen-bonded sheet all have dipole moments in almost parallel orientation at angles 35 (30)°. The sense of these dipoles is reversed in adjacent sheets.

As shown in Table II, calculated energies for the dimers in the crystal complex seem physically reasonable but have marginal significance in terms of their esds. Thus, two different doubly hydrogen-bonded pairs of parabanic acid and thiourea molecules have energies −19 (24) and −18 (14) kJ mol^{-1}, less than the energy −36 (21) kJ mol^{-1} for a parabanic acid dimer linked by a single hydrogen bond. Energies for the other dimers in Table II are negligible. This includes the dimer with a stacking of parabanic acid and thiourea, where the short C---S distances were treated in the same way as the short C---O distances in CO_2–H_2O and alloxan.

(f) Alloxan. Swaminathan et al.[15] have reported a multipole refinement for alloxan at 123 K, using neutron diffraction to determine atomic positional and thermal parameters. The crystal structure (Figure 7a) consists of a herringbone arrangement of nearly planar molecules, with unusually short C=O---C contacts [2.73 (1), 2.902 (1), and 2.988 (1) Å]. By contrast the hydrogen bond contacts are long [2.324 (2) and 2.352 (2) Å], each N–H group making close contacts with carbonyl groups on two adjacent molecules (i.e., the hydrogen bonds are bifurcated). Molecules in the crystal structure must be strongly bound, since alloxan sublimes at 503 K[15] and has a crystal density of 1.93 g cm^{-3} at 298 K. An atom–atom potential estimate of the crystal sublimation energy, which is unknown experimentally, is 107 kJ mol^{-1},[62]

(62) Poltev, V. I. *Int. J. Quantum Chem.* **1979**, *16*, 863–868.

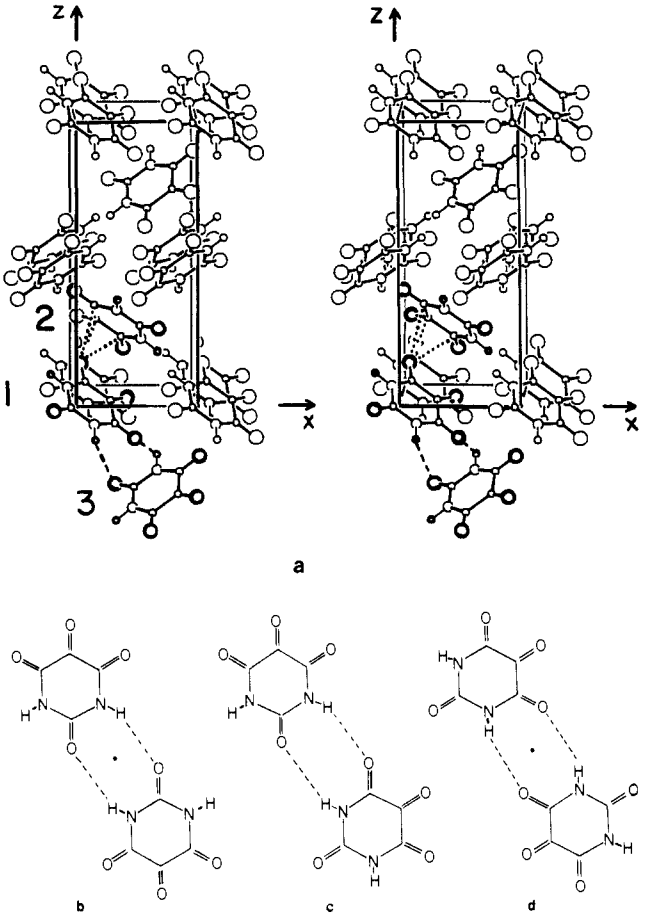

Figure 7. Alloxan, $C_4H_2N_2O_4$, space group $P2_12_12$. (a) Stereoscopic view of the molecular packing. Short —C=O---C contacts are represented by dotted lines and hydrogen bonds by dashed lines. (b,c,d) Alloxan dimers in three hypothetical configurations.

even greater than the observed value for urea.

Each molecule has eight nearest neighbors, with interactions of two types. Molecule 2 in Figure 7a forms three close C=O---C distances with molecule 1, giving an interaction energy (Table II) that is only −2 (2) kJ mol^{-1}. All three C=O---C interactions are treated as described in a previous section, by neglecting the atom–atom repulsive terms for each pair of closely separated C---O atoms. If those terms were included in the calculation, there would be a strong net repulsion.

The hydrogen bond interactions in the crystal are only weakly attractive [−5 (4) kJ mol^{-1}; Table II]. This is also true for optimized configurations of pairs of isolated alloxan molecules. We considered three possibilities for dimers linked by a pair of hydrogen bonds (Figure 7b,c,d). For the dimer in Figure 7b, we obtained an optimum energy of only −16 kJ mol^{-1} and an O---H separation of 2.31 Å (cf. 2.32 Å in the crystal). For the dimer in Figure 7c we obtained an interaction energy of −11 kJ mol^{-1} and O---H separations of 2.36 Å [O(2)---H(1)] and 2.39 Å [O(6)---H(1), cf. 2.35 Å in the crystal]. These separations are close to accepted values for van der Waals contacts. For the third pairing (Figure 7d), the binding energy is even less (−6 kJ mol^{-1}), with equilibrium O---H separations of 2.51 Å.

These results are particularly informative. They tell us that the hydrogen bond energy is small even in configurations with maximum interaction. Alloxan molecules have a limited capacity for hydrogen bonding, probably because the molecules have little polarity ($|\mu|$ = 0.2 (1.0) D in Table I). For comparison with alloxan, the optimum configuration of the cyclic urea dimer (Figure 5c), a configuration which is not observed in the crystal structure, has a binding energy −47 kJ mol^{-1}.

Therefore, we are left wondering what binds the molecules together in the crystal. We expect that we are not modeling the close C=O---C interactions particularly well. As discussed above,

the assumption that we can model such interactions by neglecting the atom-atom terms for the O---C pair is not well understood, although it appears to describe the CO_2-H_2O dimer quite well. Further theoretical work on modelling such interactions is clearly required.

Discussion and Conclusion

We have attempted to paint a picture (albeit with a very broad brush) of the sort of results that can be obtained by computing intermolecular energies from the experimental electron density distributions in molecular crystals. There are many details that deserve further consideration. However, we believe that we have achieved our principal goal. This was to demonstrate that the multipole expansion of $\rho(r)$ about the atomic nuclei, as obtained directly from diffraction data, contains valuable information about the energetics and configurations of molecular systems, particularly those that are hydrogen bonded. The advent of such a direct approach for estimating E_{es} may become useful in assessing the importance of various types of hydrogen bonding in crystals. In the past, such judgements have tended to rely heavily on various geometrical criteria involving interatomic distances and angles, such as those proposed by Hamilton and Ibers[63] and others subsequently.

However, we must be cautious in the interpretation of our results, for several reasons. First, and most obviously, the energies we have computed have associated with them quite large esds. This point has not been addressed in previous studies,[2,3,9] but it deserves consideration in the future. Values of E_{es} are proportional to products of pairs of experimentally determined $C_{lm\pm}$ parameters. Hence the relative error in a property such as E_{es} should be about double when compared with a property such as the charge density which is linearly dependent on $C_{lm}^{\pm}$. From our calculations for the crystal complex of thiourea and parabanic acid, it seems unlikely that significant values of E_{es} can be obtained from X-ray diffraction data collected at room temperature. In order to draw definitive conclusions about molecular interaction energies from diffraction data alone, high-resolution Bragg intensity data are needed at or beyond the levels of precision which are presently attainable.

Secondly, we note that the simple model used to approximate the remaining components of the interaction energy (repulsion, dispersion, polarization, charge-transfer, etc.) is far from fully optimized. The main reason it appears to work so well at present is because deficiencies are hidden by the large values of $\sigma(E_{es})$. However, we must seek a better understanding of the approximation used to describe the hydrogen bond, and in particular its extension to C=O---C type interactions, as discussed in this work.

Acknowledgment. This work was supported by Grant HL-20350 from the National Institutes of Health. We are grateful to Joan Klinger for technical assistance.

Registry No. Imidazole, 288-32-4; 9-methyladenine, 700-00-5; cytosine monohydrate, 6020-40-2; urea, 57-13-6; parabonic acid-thiourea (1:1), 58343-74-1; alloxan, 50-71-5.

(63) Hamilton, W. C.; Ibers, J. A. *Hydrogen Bonding in Solids*; Benjamin: New York, 1968.

Magnetic Ordering of $Mn^{II}Cu^{II}$ Bimetallic Chains: Design of a Molecular-Based Ferromagnet

Olivier Kahn,*† Yu Pei,† Michel Verdaguer,† Jean Pierre Renard,‡ and Jorunn Sletten§

Laboratoire de Spectrochimie des Elēments de Transition, U.A. No. 420, Universitē de Paris Sud, 91405 Orsay, France, Institut d'Electronique Fondamentale, U.A. No. 022, Universitē de Paris Sud, 91405 Orsay, France, and Department of Chemistry, University of Bergen, 5007 Bergen, Norway. *Received March 26, 1987*

Abstract: The compound $MnCu(pbaOH)(H_2O)_3$ (**2**) with pbaOH = 2-hydroxy-1,3-propylenebis(oxamato) has been synthesized, and its crystal structure has been solved. It crystallizes in the orthorhombic system, space group $P2_12_12_1$, with a = 12.351 (7) Å, b = 21.156 (11) Å, c = 5.073 (10) Å, and Z = 4 (MnCu units). The structure consists of ordered bimetallic chains running along the b axis with Mn^{II} and Cu^{II} ions bridged by oxamato groups. The shortest interchain metal-metal separations are Mn···Cu = 5.751 Å in the a direction and Mn···Mn = Cu···Cu = 5.073 Å in the c direction. The magnetic properties of **2** have been investigated and compared to those of $MnCu(pba)(H_2O)_3\cdot 2H_2O$ (**1**) with pba = 1,3-propylenebis(oxamato), which has been previously described. **1** has the same chain structure as **2**, but along the a direction the shortest separations are of the type Mn···Mn and Cu···Cu instead of Mn···Cu. In the $30 < T < 300$ K temperature range, the $\chi_M T$ versus T plots for **1** and **2** are identical and characteristic of antiferromagnetically coupled ordered bimetallic chains with a minimum of $\chi_M T$ at 115 K. Upon cooling below 30 K, $\chi_M T$ increases much faster for **2** than for **1** and diverges around 5 K. **1** orders antiferromagnetically at 2.2 K with a small canting along the a direction. In contrast, **2** orders ferromagnetically at 4.6 K. The temperature dependences of the magnetization M for **2** along the three directions of the lattice have been investigated and have shown that the c axis is the easy magnetization axis. The M versus the field H plot has also been studied for a polycrystalline sample at various temperatures between 4.2 and 1.3 K. A hysteresis loop characteristic of a soft magnet has been obtained. At 1.3 K, the remnant magnetization is 2.25×10^3 cm^3 mol^{-1} G and the coercive field around 50 G. The mechanism of the 3D magnetic ordering in **1** and **2** has been discussed. The key role has been suggested to be the relative positions of the chains along the a direction.

For a few years, we have participated in the efforts to design molecular systems ordering ferromagnetically. Molecular in this context means that we use the synthesis methods of the molecular chemistry—we work in solution, with mild conditions of temperature and pressure—and that we attempt to build the three-dimensional lattice by assembling molecular bricks in a controllable fashion. One possible approach along this line consists of synthesizing molecular entities with a large spin multiplicity in their ground state and then of assembling them within the crystal lattice in a ferromagnetic fashion.[1-3] A slightly different approach

† Laboratoire de Spectrochimie des Elēments de Transition, Universitē de Paris Sud.
‡ Institut d'Electronique Fondamentale, Universitē de Paris Sud.
§ University of Bergen.

(1) Iwamura, H.; Sugawara, T.; Itoh, K.; Takui, T. *Mol. Cryst. Liq. Cryst.* **1985**, *125*, 251.

0002-7863/88/1510-0782$01.50/0